Non-Destructive Testing by ultrasound for multi-pass austenitic welds. Influence of the uncertainty of elastic constants on the detection of a defect

Cécile Gueudré, Jean Mailhé, Marie-Aude Ploix, Gilles Corneloup

Non-Destructive Testing by ultrasound for multi-pass austenitic welds. Influence of the uncertainty of elastic constants on the detection of a defect

C. GUEUDRE [1], J. MAILHE [1], M.A. PLOIX [1], G. CORNELOUP [1,a]

[1] Aix Marseille Université, CNRS, Centrale Marseille,
LMA, UMR 7031, 4 impasse Nikola Tesla, CS 40006
13453 Marseille Cedex 13, France

[a]gilles.corneloup@univ-amu.fr

Abstract

Ultrasonic testing of austenitic stainless steel multi-pass welds is complex. Because of the welded structure both anisotropic and heterogeneous, the propagation of the ultrasonic beam is disrupted (attenuation, deviation, division), making diagnosis difficult.

This diagnosis can be improved by modelling the propagation. For this purpose, a description of the microstructure is required. This can be obtained by macrography, but this involves a destructive cutting of the weld, or a weld sample. In the latter case, the sample must have been made and stored, and it must be representative of the inspected weld.

As an alternative, since 2000, EDF and the LMA have been developing a numerical model (called MINA) for predicting the microstructure of SMAW multi-pass welds, which only takes into account information from welding conditions. It is then coupled to the ATHENA ultrasonic simulation code, developed by EDF R&D, to simulate the impact of welding on propagation and therefore control.

In certain cases, some discrepancies are observed between simulation and experimentation. This study (as part of the MUSCAD ANR Project) shows that they can be partly attributed to the measurement uncertainties of the elasticity constants Cij (relevant model input data) of the welded metal.

The analytical uncertainty propagation method is used to quantify the influence of Cij variability on the propagation simulation result. The deviation in position and in time of flight of a classical ultrasonic test (NDT) is clearly shown.

Keywords: Ultrasound, multi-pass weld, modelling, uncertainty, elasticity constants

1. Introduction

The primary circuit in pressurized water reactors includes numerous components, such as the vessel, the steam generator, the primary pumps, the pressurizer, interconnected by a piping system conveying high pressure, high temperature water. Most of these components are made of austenitic stainless steel, as it exhibits excellent corrosion resistance and very good mechanical strength at high temperature. Non-destructive tests aim at detecting potential defects in the numerous multi-pass welds present in the primary circuit and at characterizing them (position and dimensions), so that their severity can be assessed.

Ultrasonic testing makes it possible to detect and characterize defects whatever their orientation, but the results may be problematic to interpret, especially for these complex thick welds. A realistic prediction of the microstructure should provide valuable insight into ultrasonic propagation through those complex structures and thereby allow a better controllability.

The non-destructive ultrasonic testing of such welds reveals phenomena of deviation and division of the ultrasound beam generated by the structure, as well as attenuation and structure noise [1,2].

Numerous simulation codes of ultrasonic propagation are available in the literature to address the problem of ultrasonic testing of polycrystalline metals with both anisotropic and heterogeneous structures. Many of them are based on ray-tracing methods [3,4] because they are less expensive in computation time than finite element methods (FEM). ATHENA code used here and developed by EDF is a finite element code that solves the elastodynamic equations, in the transient regime, in a heterogeneous and anisotropic medium [5].

Whatever the chosen code, the simulation requires a realistic description of the weld as input data. The models of grain structure at the macroscopic scale often use simplified symmetrical descriptions [3,4]. The LMA has developed a welding model named MINA (Modeling anIsotropy from Notebook of Arc welding) [6], which provides the microstructure of a weld, with no need for cutting. This model, created for shielded metal arc welding (SMAW) in flat position, allows good prediction of the grain orientation [7]. It uses information from the welding notebook (describing the welding procedure), and the rules related to crystal growth and specific welding process parameters. The elasticity constants are then assigned to these orientations and the modelling of ultrasonic propagation can be performed.

ATHENA uses as input data the description of the weld, and the elastic constants Cij of the material, for which experimental measurements on calibrated workpieces have shown they have certain variability. How this variability affects the simulation results is studied in this paper. And the consequences of Cij uncertainty are discussed in terms of Non-Destructive Testing, in

particular how it influences the position and the time of flight of the amplitude maximum according to the position of the transducer.

2. Modelling of ultrasound propagation through anisotropic heterogeneous welds

The heterogeneous and anisotropic weld is described in ATHENA by a finite number of homogeneous orthotropic domains (meshes). Each domain has its own local grain orientation, so that the propagation code can deduce the orientation of the coordinate systems of the elasticity constants in each point of the weld.

The weld selected for this study is an austenitic stainless steel multi-pass weld made by a manual process of shielded metal arc welding, in horizontal position (that is to say, horizontal welding of two vertical pieces). Here, the orientations of the grains in the weld (see Figure 1a below) are obtained from macrographic analysis to remove any doubt about possible error on this input data.

In order to obtain the Cij values, seven homogeneous, orthotropic samples with different grain orientations (from 0° to 90°, 15° increment) were cut out from a weld mock-up. The tensor of the elasticity constants of a homogeneous orthotropic material is composed of 9 independent elasticity constants. As far as simulations are performed in 2D, we will only consider the 4 Cij involved. They are given in Table 1. They were determined [8] from a measurement of velocities associated with an optimization algorithm in the framework of a previous project ANR MOSAICS [9].

	C11	C33	C13	C55
mean	242.9	230.9	142.9	110.0
standard deviation	18	8	6	5.5

Table 1. Elasticity constants (GPa) of the welded austenitic stainless steel, where the axis of crystallographic texture <100> corresponds to axis 3 (2D case)

Figure 1b represents the "beam tracing" which is actually the norm of maximum velocity reached at each node of the mesh during the FEM simulation.

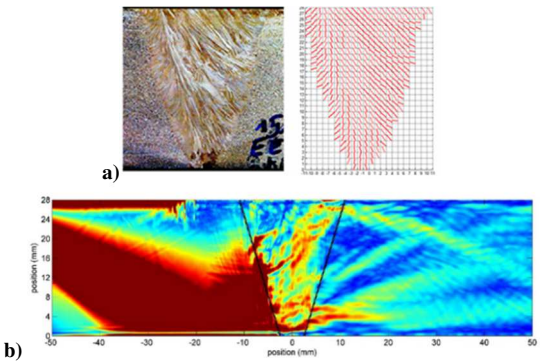

Figure 1. a) Macrography and orientations of the studied horizontal weld, b) Energy propagation for the position of the transmitter 70mm from the centre axis of the weld (P70). Image deliberately saturated to enhance contrast in the area of interest.

It shows perfectly the disturbances of the ultrasonic beam through a heterogeneous anisotropic weld.

This configuration is chosen as starting configuration, because of its great sensitivity to the highly dissymmetric orientations present in the weld, here a horizontal welding of two vertical pieces and a T60 testing beam (transverse waves at 60° generated by a phased array transducer).

3. Method of analytical propagation of uncertainties

The method of analytical propagation of uncertainties is used here to study the ultrasonic simulation sensitivity to the uncertainties of the Cij. For a given position of the transmitter and a given acquisition mode (T60), this method makes it possible to determine, in a defined domain of the weld, the influence of the uncertainty of the Cij on the result of the simulation.

The analytical uncertainty propagation method makes it possible to test a great number of possible acquisition configurations (acquisition mode, position of the transmitter, descriptor) in a short space of time (unlike a method of the Monte Carlo type for example).

The parametric descriptor used is the seismogram (figure 2). It is like a Bscan representation, in the {space; time} domain, but corresponding to the time signals recorded by each element in the linear receiver array at the surface of the part (the transducer does not act as a transmitter/receiver, unlike the Bscan case).

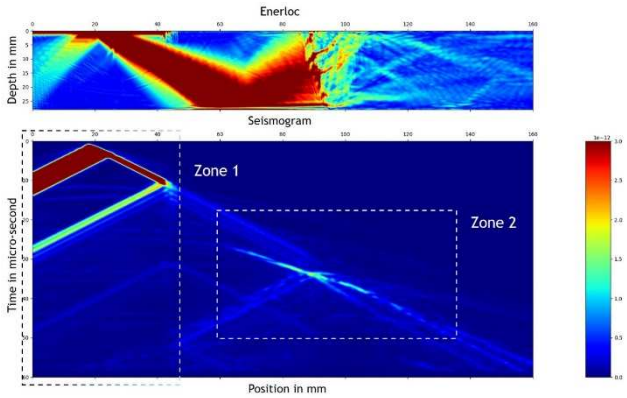

Figure 2. Ultrasonic propagation and seismogram for configuration T60 and position P70 of the emitter. Images voluntarily saturated to enhance propagation through weld

This seismogram is composed of 2 different zones. Zone 1 is not accessible experimentally. It is possible to visualize the emission as well as the surface waves and their reflection by the artificial cracks (inserted to block these artefact waves). Zone 2 is the region of interest, where the ultrasonic waves are received after passing through the weld. In the following, the results will be plotted only in this zone.

4. Creation of the maps of sensitivities for each Cij

The analytical uncertainty propagation equation indicates that the variances $\sigma^2_{s_{mn}}$ of the simulation results (seismogram) are equal to the product of the gradient, noted $\vec{\nabla}S_{mn}$, of the amplitude S at a point (m,n) of the seismogram with respect to the Cij values, representing the sensitivities of the model to the Cij and the covariance matrix of the Cij:

$$\sigma^2_{s_{mn}} = \vec{\nabla}S^T_{nm} \cdot cov(C_{ij}) \cdot \vec{\nabla}S_{mn} \quad (1)$$

With $cov(C_{ij}, C_{kl}) = \Sigma_{n=1}^{nb} \frac{(\overline{C_{ij}}_n - {C_{ij}}_n)(\overline{C_{kl}}_n - C_{kl_n})}{nb-1}$ (2)

where nb is the number of experimental measurements of Cij.

The method [10] includes three notions (cf. figure 3):

- the covariance matrix of the measured Cij (and their uncertainties),
- the gradients of the amplitudes of the simulated seismogram depending on each Cij (sensitivity maps),
- the variances of the amplitudes of the simulated seismogram taking account of standard deviations of all the Cij (uncertainty map).

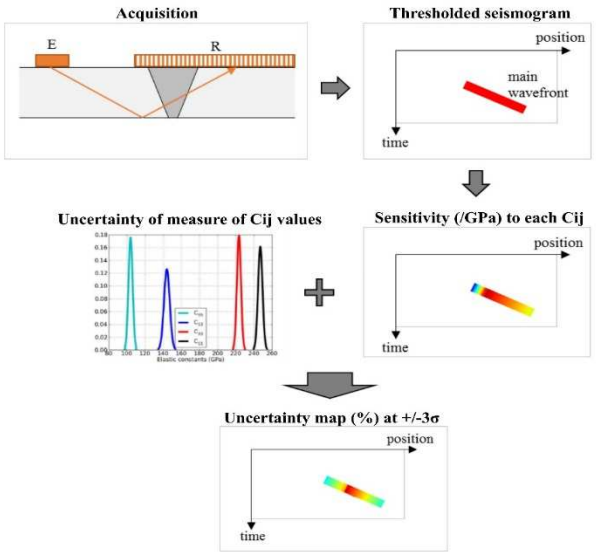

Figure 3. Schematic diagram of the method principle

The sensitivity to a given Cij corresponds to the partial derivative of the amplitude of each point on the seismogram.

For each point on the seismogram, a sensitivity to a particular Cij is thus calculated, and is represented, in the same coordinate system, in the form of a sensitivity map to one Cij (figure 4).

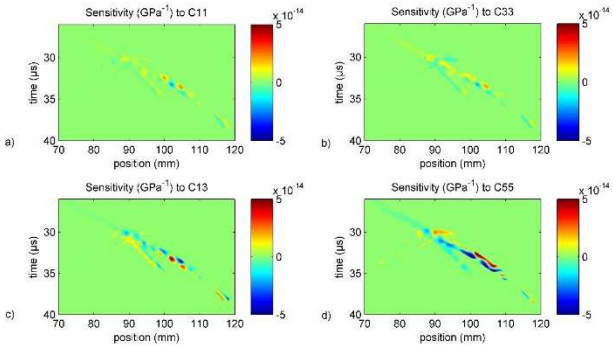

Figure 4. Maps of amplitude sensitivities (GPa^{-1}) to the Cij (Cij variation from -σ_{Cij} to +σ_{Cij} of Table 1, T60, P70)

5. Creation of the map of uncertainties due to the variations of all Cij

Multiplying model sensitivities to the Cij by the variance-covariance matrix of the Cij, one obtains the variances of the simulation results (equation 1), which are represented under the form of an uncertainty map. The uncertainty corresponds to the containment of the possible error on the simulated ultrasonic amplitude. It is calculated according to the equation:

$$uncertainty(x,t) = \pm 3 \cdot \sqrt{{\sigma_{S_{nm}}}^2} \quad (3)$$

The map of the amplitude uncertainties due to the variations of the elastic constants (figure 5) gives the influence of the variation of all the Cij simultaneously, this time taking into account their own standard deviations.

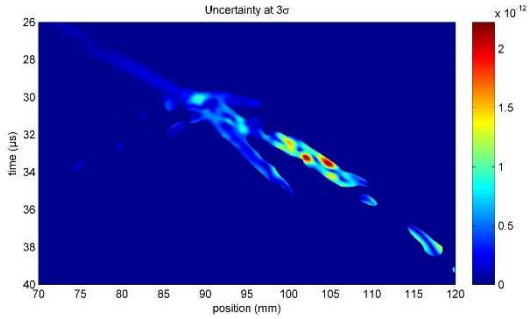

Figure 5. Map of amplitude uncertainties (T60, P70) due to the variations of all the Cij within ranges of Table 1

6. Discussion on the consequences for NDT

In conventional industrial NDT, the location of a detected defect, its nature and its dimensions, can be obtained by studying the propagated acoustic beam. The principle remains the same: the position of the maximum ultrasonic amplitude is sought. This position corresponds to the theoretical axis of the propagated beam if there is no deviation of the beam (isotropic material), and if the input data in terms of ultrasonic velocity are those of the material.

Otherwise, there will be a gap. Confidence in the control performed can be given if one is able to relate this deviation of the beam to the characteristics of anisotropy and heterogeneity of the material. It is therefore necessary that these are perfectly known.

Our study shows that the uncertainty about the knowledge of these characteristics, therefore of the Cij, not only has a negative consequence on the control simulations of a weld, but also that this consequence is different according to the controlled weld zones.

Focusing on the maximum amplitude point of the main wavefront on the seismogram, for position P70 (fig.2), the displacement of this maximum point in position ($disp_x$) and in time ($disp_t$), caused by the variation of each Cij, can be noted. The results obtained are presented in Table 2 and they show that for this control position, the uncertainty on the Cij has practically no effect.

Displacements of the maximum amplitude point				
	C11	C33	C13	C55
$disp_x$ (mm)	0	0	0.1	0.1
$disp_t$ (µs)	0.05	0.03	0.03	0.02

Table 2. Displacements in position and in time of the maximum amplitude point of the main wavefront (Cij variation from $-\sigma_{Cij}$ to $+\sigma_{Cij}$ of Table 1, T60, P70)

Conversely for position P30 (transmitter positioned at 30mm from the centre axis of the weld), we show that the displacements, in position and in time, of the maximum amplitude point of the main wavefront are far greater (Table 3). The variation of a Cij can cause a significant displacement of the echo (for example here, up to about 8 mm and 2.5 µs) and thereby lead to false NDT diagnosis.

Indeed, a deviation greater than 2-3 mm in the position of the amplitude maximum and/or a difference of 1 µs are sufficient to disturb the controller. He/she no longer understands the propagation of the beam, and he/she can't reliably decide for example if an echo corresponds to a defect or to a specific geometry of the sample.

Displacements of the maximum amplitude point				
	C11	C33	C13	C55
$disp_x$ (mm)	8.3	4.1	3.9	0.7
$disp_t$ (µs)	2.56	1.25	1.25	0.26

Table 3. Displacements in position and time of the maximum amplitude point of the main wavefront (Cij variation from $-\sigma_{Cij}$ to $+\sigma_{Cij}$ of Table 1, T60, P30)

7. Conclusions and perspectives

This study has made it possible to quantify the influence of the precise knowledge of the Cij on the ultrasonic propagation simulation, this influence being highly dependent on the testing conditions (position of the sensors relative to the weld). It clearly demonstrates that conventional non-destructive testing (consisting of searching the evolution for echo maxima) will be influenced and disturbed by the beam deviation, and the change in time of flight .

The only way to reduce this disturbance is the most precise knowledge possible of Cij. This can be done through a specific characterization procedure of the controlled materials. But here we show the limits obtained when, in industrial conditions, we use a database of Cij recorded for a wide range of materials. Indeed elasticity constants generally used are taken from the literature and they are not exactly in accordance with the tested specimen.

Further study will be also carried out on the influence of the uncertainty of the imaginary part of the Cij, very difficult to measure, and whose effect on the modelled attenuation will be significant.

Acknowledgements

This work was realized in the framework of the MUSCAD (Méthodes UltrasonoreS pour la Caractérisation de matériaux de composants nucléaires pour l'Amélioration du Diagnostic) project which is supported by the French National Agency of Research.

References

[1] G. Corneloup, C. Gueudré, Non Destructive Testing and testability of materials and structures (Le contrôle non destructif et la contrôlabilité des matériaux et structures), PPUR, 2016.

[2] B. Chassignole, R. El Guerjouma, M.-A. Ploix, T. Fouquet, Ultrasonic and structural characterization of anisotropic austenitic stainless steel welds: Towards a higher reliability in ultrasonic non-destructive testing, NDTE Int. 43 (2010) 273–282. doi:10.1016/j.ndteint.2009.12.005.

[3] J.A. Ogilvy, Computerized Ultrasonic Ray Tracing in Austenitic Steel, NDTE Int. 18(1985) 67–77. doi:10.1016/0308-9126(85)90100-2.

[4] O. Nowers, D.J. Duxbury, B.W. Drinkwater, Ultrasonic array imaging through an anisotropic austenitic steel weld using an efficient ray-tracing algorithm, NDTE Int. 79 (2016) 98–108. doi:10.1016/j.ndteint.2015.12.009.

[5] [12] B. Chassignole, V. Duwig, M.-A. Ploix, P. Guy, R. El Guerjouma, Modelling the attenuation in the ATHENA finite elements code for the ultrasonic testing of stainless steel welds, Ultrasonics. 49 (2009) 653–658. doi:10.1016/j.ultras.2009.04.001

[6] J. Moysan, A. Apfel, G. Corneloup, B. Chassignole, Modelling the grain orientation of austenitic stainless steel multipass welds to improve ultrasonic assessment of structural integrity, Int. J. Press. Vessels Pip. 80 (2003) 77–85. doi:10.1016/S0308-0161(03)00024-3.

[7] Z. Fan, M.J.S. Lowe, Investigation of Ultrasonic Array Measurements to Refine Weld Maps of Austenitic Steel Welds, Rev. Prog. Quant. NDE. Vols 31a 31b. (2012) 873–880.

[8] N. Alaoui-Ismaili, P. Guy, B. Chassignole, Experimental Determination of the Complex Stiffness Tensor and Euler Angles in Anisotropic Media Using Ultrasonic Waves, Rev. Prog. Quant. NDE. Inc. 10th Int. Conf. Barkhausen Noise Micromagnetic Test. Vols 33a 33b. (2014) 934–940. doi:10.1063/1.4864921.

[9] B. Chassignole, P. Recolin, N. Leymarie, C. Gueudre, P. Guy, D. Elbaz, Study of Ultrasonic Characterization And Propagation In Austenitic Welds: The MOSAICS Project, Rev. Prog. Quant. NDE Vol 34. (2015) 1486–1495. doi:10.1063/1.4914766

[10] C. Gueudré, J. Mailhé, M.A. Ploix, G. Corneloup, B. Chassignole, Influence of the uncertainty of elastic constants on the modelling of ultrasound propagation through multi-pass austenitic welds. Impact on nondestructive testing, Int. J. Press. Vessel. Pip. 171 (2019) 125-136. doi: 10.1016/j.ijpvp.2019.02.011